International Journal of Innovation in Science and Mathematics
Volume 3, Issue 3, ISSN (Online): 2347–9051

Effect of Radiation, Heat Source, Viscous Dissipation on Heat and Mass Transfer of Nanofluid Over a Nonlinear Stretching Sheet

Dr. V. Dhanalaxmi
Department of Mathematics, University College of Technology,
Osmania University, Hyderabad, 500007, India.
Email: v_laxmi_sudha@yahoo.co.in

Abstract **– The present paper focuses on free convective boundary layer flow of a radiating nanofluid along a non-linear stretching sheet. The model used for the nanofluid incorporates the effects of Brownian motion and thermophoresis. The governing boundary layer equations are reduced into ordinary differential equations by a similarity transformation. The transformed equations are solved numerically using Rungekutta fourth order method along with shooting technique. The numerical predictions have been compared with existing information in the literature [21] & [22] and good agreement is obtained. The effects of various parameters on velocity, temperature and concentration profiles are presented graphically and discussed. Numerical values of skin friction coefficient, Nusselt numbers and the Sherwood numbers are presented in tabular form.**

Keywords **– Nanofluid, Heat Transfer, Viscous Dissipation, Internal Heat Generation, Radiation.**

I. INTRODUCTION

Studies related to nanofluids have attracted a great deal of interest in recent time due to their enormous enhanced performance properties, particularly with respect to heat transfer. Nanofluids have *novel* properties that make them potentially useful in many applications in heat transfer, including microelectronics, fuel cells, pharmaceutical processes and hybrid-powered engines. Nano particle is of great scientific interest as it is an effectively bridge between bulk materials and atomic or molecular structures. Nanofluids are characterized by an enrichment of a base fluid like water, toluene, ethylene glycol or oil with nano particles in variety of types like metals, oxides, carbides, carbon, nitrides etc.

An innovative technique, which uses a mixture of nano particles and the base fluid, was first introduced by Choi [1] in order to develop advanced heat transfer fluids with substantially higher conductivities. Later Das et al. [2] experimentally showed a two-to four-fold increase in thermal conductivity enhancement for water-based nanofluids containing Al_2O_3 or CuO nano particles over a small temperature range $21^0 - 51^0$c. Buongiorno[3] gave a satisfactory explanation for the abnormal increase of the thermal conductivity. Buongiorno and Hu [4], investigated on the nanofluid coolants in advanced nuclear systems. Mixed convection boundary layer flow from a vertical flat plate embedded in a porous medium filled with nanofluids was investigated by Ahmad and Pop [5]. Hady et al. [6] investigated the effects of thermal radiation on the viscous flow of a nanofluid and heat transfer over a non-linearly stretching sheet. Olanrewaju et al. [7] studied the boundary layer flow of nano fluids over a moving surface with radiation effects. Hamid et al. [8] analyzed the radiation effects on Marangoni boundary layer flow past a flat plate in a nano fluid. EI-Aziz [9] studied radiation effect on the flow and heat transfer over an unsteady stretching surface. Singh et al. [10] investigated the thermal radiation and magnetic field effects on an unsteady stretching permeable sheet in the presence of free stream velocity. Gbadeyan et al. [11] studied the boundary layer flow of a nano fluid past a stretching sheet with convective boundary conditions in the presence of magnetic field and thermal radiation. Ibrahim [12] investigated the radiation effects on MHD free convection flow along a stretching surface with viscous dissipation and heat generation. Manna et al. [13] studied the effects of radiation on unsteady MHD free convective flow past an oscillating vertical porous plate. Anandrao et al. [14] investigated the radiation effect on an unsteady MHD free convective flow past a vertical porous plate.

Very recently, Kuznetsov and Nield [15] have examined the influence of nano particles on the natural convection boundary layer flow past a vertical plate incorporating Brownian motion and Thermophoresis treating both the temperature and the nano particles fraction as constant along the wall. Further, Nield and Kuznetsov [16] have studied the problem proposed by Cheng and Minkowycz [17] about the natural convection past a vertical plate in porous medium saturated by a nano fluid taking into the account the Brownian motion and thermo phoresis. Ali Pakranravan and Yaghoubi [18] studied the combined thermophoresis ,Brownian motion and Dufour effects on natural convection of nano fluids. All these researchers studied linear stretching sheet in the nano fluid, but a numerical investigation was done by Rana and Bhargava [19] who studied the steady laminar boundary fluid flow of nano fluid past a nonlinear stretching flat surface with the effects of Brownian motion and thermoporesis. Also recently Nadeem and Lee [20] investigated analytically the problem of steady boundary layer flow of nano fluid over an exponentially stretching surface including the effects Brownian motion parameter and thermophoresis parameter. Poornima and Reddy [21] studied simultaneous effects of thermal radiation and magnetic on heat and mass transfer flow of nanofluids over a non-linear stretching sheet.

To the best of author's knowledge, so far effect of radiation, viscous dissipation and heat source on heat and

mass transfer on free convective boundary layer flow nanofluid past a non-linear stretching sheet has not been investigated. So the aim of present paper is to study the effect of radiation, internal heat generation on viscous flow of a nanofluid over a non-linear stretching sheet. The governing boundary layer equations are reduced to a system of nonlinear ordinary differential equations using similarity transformations and the resulting equations are solved numerically by using Rungekutta fourth order method along with shooting technique. A parametric study is conducted to illustrate the influence of various governing parameters on the velocity, temperature, concentration profiles. Skin friction coefficient, Nusselt number and Sherwood number are discussed in detail.

II. MATHEMATICAL ANALYSIS

A steady two-dimensional boundary layer flow of an incompressible radiating nanofluid past a stretching surface is considered under the assumptions that the external pressure on the stretching sheet in the x-direction is having diluted nanoparticles. The x- axis is taken along the stretching surface and y- axis normal to it.

A uniform stress leading to equal and opposite forces is applied along the x- axis so that the sheet is stretched, keeping the origin fixed. The stretching velocity is assumed to be $U_w(x) = U_0x^m$ where U_0 the uniform velocity and m($m\geq 0$) is a constant parameter. The fluid is considered to be a gray, absorbing emitting radiation but non- scattering medium. Employing the Oberbeck-Boussinesq approximation, the governing equations of the flow field can be written in the dimensional form (Anwar M I, Khan I [22], Kuznetsov AV, Nield DA[23], Khan WA, Pop I [24]) as

$$\frac{\partial u}{\partial x}+\frac{\partial u}{\partial y}=0 \tag{1}$$

$$\frac{\partial p}{\partial x}=\mu\frac{\partial^2 u}{\partial y^2}-\rho_f\left(u\frac{\partial u}{\partial x}+v\frac{\partial u}{\partial y}\right)+\left[(1-C_\infty)\rho_{f_\infty}\beta_T(T-T_\infty)-\left(\rho_p-\rho_{f_\infty}\right)\beta_C(C-C_\infty)\right] \tag{2}$$

$$u\frac{\partial T}{\partial x}+v\frac{\partial T}{\partial y}=\alpha\nabla^2 T+\tau\left\{D_B\left(\frac{\partial T}{\partial y}\frac{\partial C}{\partial y}\right)+\frac{D_T}{T_\infty}\left(\frac{\partial T}{\partial y}\right)^2\right\}-\frac{1}{(\rho C_p)_f}\frac{\partial q_r}{\partial y}+\frac{Q}{\rho c_p}(T-T_\infty)+\frac{\mu}{\rho c_p}\left(\frac{\partial u}{\partial y}\right)^2 \tag{3}$$

$$u\frac{\partial C}{\partial x}+v\frac{\partial C}{\partial y}=D_B\frac{\partial^2 C}{\partial y^2}+\frac{D_T}{T_\infty}\frac{\partial^2 T}{\partial y^2} \tag{4}$$

The associated boundary conditions are:

$$u=U_w(x)=U_0x^m, v=0, T=T_w, C=C_w \text{ at } y=0 \; u\to 0, v\to 0, T\to T_\infty, C\to C_\infty \text{ as } y\to\infty \tag{5}$$

where *u* and *v* are the velocity components in the *x* and *y* – directions, respectively, g is the acceleration due to gravity, μ- the viscosity, ρf - the density of the base fluid, *p* – the density of the nanoparticle, β_T - the coefficient of volumetric thermal expansion, β_C - the coefficient of volumetric concentration expansion, T - the temperature of the nanofluid, C- the concentration of the nanofluid, T_w and C_w - the temperature and concentration along the stretching sheet, T_∞ and C_∞- the ambient temperature and concentration , D_B- the Brownian diffusion coefficient, D_T - the thermophoresis coefficient, q_r - radiative heat flux, *k* – the thermal conductivity, $(\rho C)_p$ - the heat capacitance of the nanoparticles, $(\rho C)_f$ - the heat capacitance of the base fluid, $\alpha = k/(\rho C)_f$ is the thermal diffusivity parameter and $\tau = (\rho C)_p/(\rho C)_f$ is the ratio between the effective heat capacity of the nanoparticles material and heat capacity of the fluid.

By using the Rosseland approximation (Brewster [25]), the radioactive heat flux q_r is given by

$$q_r=-\frac{4\sigma_s}{3k_e}\frac{\partial T^4}{\partial y} \tag{6}$$

where σ_s is the Stephen Boltzmann constant k_e is the mean absorption coefficient.

It should be noted that, the present analysis is limited to optically thick fluids. If the temperature differences within the flow are sufficiently small, then equation (6) can be linearised by expanding T^4 into the Taylor series about T_∞, which after neglecting higher order terms takes the form

$$T^4\cong 4T^3{}_\infty T-3T_\infty{}^4 \tag{7}$$

Then the radiation term in equation (3) takes the form

$$\frac{\partial q_r}{\partial y}=\frac{16\sigma_s T^3{}_\infty}{3k_e}\frac{\partial^2 T}{\partial y^2} \tag{8}$$

Invoking equation (8), equation (3) gets modified as

$$u\frac{\partial T}{\partial x}+v\frac{\partial T}{\partial y}=\left(\frac{k}{(\rho C_p)_f}+\frac{16\sigma_s T^3{}_\infty}{3k_e(\rho C_p)_f}\right)\frac{\partial^2 T}{\partial y^2}+\tau\left\{D_B\left(\frac{\partial T}{\partial y}\frac{\partial C}{\partial y}\right)+\frac{D_T}{T_\infty}\left(\frac{\partial T}{\partial x}\right)^2\right\}+\frac{Q}{\rho c_p}(T-T_\infty)+\frac{\mu}{\rho c_p}\left(\frac{\partial u}{\partial y}\right)^2 \tag{9}$$

Using the stream function $\psi=\psi(x,y)$, the velocity components *u* and *v* are defined as

$$u=\frac{\partial\psi}{\partial y} \text{ and } v=-\frac{\partial\psi}{\partial x}$$

Assuming that the external pressure on the plate, in the direction having diluted nanoparticles, to be constant, the similarity transformations are taken as

$$\psi=\sqrt{\frac{2\upsilon U_0x^{m+1}}{m+1}}f(\eta),\quad \theta(\eta)=\frac{T-T_\infty}{T_w-T_\infty},$$

$$\phi(\eta)=\frac{C-C_\infty}{C_w-C_\infty},\qquad \eta=y\sqrt{\frac{(m+1)U_0x^{m-1}}{2\upsilon}}$$

$$Nr=\frac{k_ek}{4\sigma_s T^3{}_\infty},R=\frac{4}{3Nr},\lambda=\frac{Gr}{Re_x^{\frac{3}{2}}},$$

$$\delta=\frac{Gm}{Re_x^{\frac{3}{2}}},Pr=\frac{\upsilon}{\alpha},Le=\frac{\upsilon}{D_B},\upsilon=\frac{\mu}{\rho_f}$$

$$b=\frac{\tau D_B}{\upsilon}(C_w-C_\infty),Nt=\frac{\tau D_T}{\upsilon T_\infty}\left((T_w-T_\infty)\right),$$

$$Re_x=\frac{u_w(x)\,x}{\upsilon} \tag{10}$$

$$Gr=\frac{(1-C_\infty)\left(\frac{\rho_{f_\infty}}{\rho_f}\right)gn\,(T_w-T_\infty)}{\upsilon^2Re_x^{\frac{1}{2}}},$$

$$Gm=\frac{\left(\frac{\rho_{p-}\rho_{f_\infty}}{\rho_f}\right)gn_1(C_w-C_\infty)}{\upsilon^2Re_x^{\frac{1}{2}}}$$

$$Ec = \frac{{U_0}^2 x^{2m}}{c_p(T_w - T_\infty)}, \gamma = \frac{2Q}{(m+1)\rho_{c_p} U_0 x^{m-1}}$$

In view of the above similarity transformations, the equations (2) – (4) reduce to

$$f''' + ff'' - \frac{2m}{m+1} f'^2 + \frac{2}{m+1}(\lambda\theta - \delta\phi) = 0 \quad (11)$$

$$\frac{1}{Pr}(1+R)\theta'' + f\theta' + Nb\theta'\phi' + Nt\theta'^2 + Ecf''^2 + \gamma\theta = 0 \quad (12)$$

$$\phi'' + Lef\phi' + \frac{Nt}{Nb}\theta'' = 0 \quad (13)$$

where λ is the buoyancy parameter, δ is the solutal buoyancy parameter, Pr is the Prandtl number, Le is the Lewis number, V is the kinematic viscosity of the fluid, *Nb* is the Brownian motion parameter, *Nt* is the thermophoresis parameter, Re_x is the local Reynolds number based on the stretching velocity, *Gr* is the local thermal Grashof number, *Gm* is the local concentration Grashof number and *f, θ,Φ* are the dimensionless stream functions, temperature, rescaled nanoparticle volume fraction respectively. Here, β_T and βc are proportional to x^{-3}, that is $\beta_T = nx^{-3}$ and $\beta_C = n_1 x^{-3}$, where *n* and n_1 are the constants of proportionalities (Makinde and Olanrewaju [26]).

The corresponding boundary conditions are:

$$f = 0, f' = 1, \theta = 1, \phi = 1 \; at \; \eta = 0$$

$$\theta \to 0, \phi \to 0 \; as \; \eta \to \infty \quad (14)$$

For the type of boundary layer flow under consideration, the skin- friction coefficient, Nusselt number and Sherwood number are important physical parameters. Knowing the velocity field, the shearing stress at the plate can be obtained, which in the non-dimensional form (skin-friction coefficient) is given by

$$C_f = \frac{2\tau_w}{\rho U^2} = \frac{2\mu}{\rho {U_0}^2}\left(\frac{\partial u}{\partial y}\right)_{y=0} = \frac{-1}{\sqrt{2(m+1)}} Re_x^{\frac{1}{2}} f''(0)$$

Knowing the temperature field, the heat transfer coefficient at the plate can be obtained, which in the non-dimensional form, in terms of the Nusselt number, is given by

$$Nu = \frac{q_w x}{k(T_w - T_\infty)} = -\frac{q_w}{(T_w - T_\infty)}\left(\frac{\partial T}{\partial y}\right)_{y=0}$$

$$= -\sqrt{\frac{2}{(m+1)}} Re_x^{-1/2} \theta'(0) \quad (16)$$

Knowing the concentration field, the mass transfer coefficient at the plate can be obtained, which in the non-dimensional form, in terms of Sherwood number, is given by

$$Sh = \frac{q_m x}{k(C_w - C_\infty)} = -\frac{q_m}{(C_w - C_\infty)}\left(\frac{\partial C}{\partial y}\right)_{y=0}$$

$$= -\sqrt{\frac{2}{(m+1)}} Re_x^{-1/2} \varphi'(0) \quad (17)$$

III. Numerical Solution

Since equations (11) – (13) are highly non-linear, it is difficult to find the closed form solutions. Thus, the solutions of these equations with the boundary conditions (14) are solved numerically using Rungekutta fourth order method along with shooting technique. Skin friction coefficients, Nusselt number and Sherwood number, which are respectively proportional to f " (0), -θ' (0) and -Φ' (0) are also sorted out and their numerical values are presented in tabular form.

IV. Results and Discussions

To provide a physical insight into the flow problem, comprehensive numerical computations are conducted for various values of parameters that describe the flow characteristics and the results are illustrated graphically. The value of Pr is chosen as 0.71 which corresponds to air. The values of Sc are chosen such that they represent Helium (0.3), water vapor (0.62) and Ammonia (0.78). The other parameters are chosen arbitrarily. The present results are compared with that of T. Poornima et al. [21] Anwar et al. [22] and in the absence of porosity, viscous dissipation and heat source and found that there is an excellent agreement (TABLE: 1).

The transformed nonlinear ordinary differential equations (11) – (13) subject to the boundary conditions (14) were solved numerically using Rungekutta fourth order method along with shooting technique. Velocity, temperature and concentration profiles are obtained for various values of governing parameters, and these results are used to compute the skin friction coefficient the Nusselt number and Sherwood number in equations. The effect of various governing parameters on the skin friction coefficient -f " (0), Nusslet number -θ' (0) and Sherwood number -Φ' (0) is shown in Table 2. It is observed that -θ' (0) decreases with increasing values of Nb, Nt, m and δ, whereas it is an increasing function of Pr, Le and λ. However, it is found that -θ' (0) decreases for larger values of Nt,Pr, δ and m, whereas it increases for increasing values of Nb, Le, λ. It is further observed that skin friction coefficient is an increasing function of Nt, Pr, δ and m, whereas it decreases with increasing values of Nb, Le and λ.

Table 1: Comparison of reduced Nusslet number, reduced Sherwood number with $Ec = 0, \gamma = 0$.

Nb	Nt	Pr	Le	λ	δ	m	Poornima Reddy [21]	Anwar & Khan et al. 2012 [22]	Present results
							-θ'(0)-Φ'(0)	-θ'(0)-Φ'(0)	-θ'(0)-Φ'(0)
0.1	0.1	10	10	0	0	1	0.952376 2.12939	0.9524 2.1294	0.952402 2.129444
0.2	0.2						0.365357 2.51522	0.3654 2.5152	0.365302 2.515377
0.3	0.3						0.135514 2.60881	0.1355 2.6088	0.135429 2.608999
0.4	0.4						0.049465 2.60384	0.0495 2.6038	0.49389 2.604008
0.5	0.5						0.017922 2.5731	0.0179 2.5731	0.017868 2.573240

International Journal of Innovation in Science and Mathematics
Volume 3, Issue 3, ISSN (Online): 2347–9051

Table 2: Computations of the skin friction coefficient, Nusselt number and the Sherwood number for various physical parameters.

R	Ec	γ	Pr	Nb	Nt	Le	m	δ	λ	-f ''(0)	-θ'(0)	-Φ'(0)
0.2	0.1	0.1	0.71	0.1	0.1	10	1	1	1	0.8584	0.3513	2.3007
0.2	0.1	0.1	0.71	0.1	0.1	10	1	1	1	1.0782	0.3211	2.2602
0.4	0.1	0.1	0.71	0.1	0.1	10	1	1	1	0.8399	0.3275	2.3122
0.2	0.2	0.1	0.71	0.1	0.1	10	1	1	1	0.8545	0.3411	2.3066
0.2	0.1	0.2	0.71	0.1	0.1	10	1	1	1	0.8301	0.2810	2.3422
0.2	0.1	0.1	0.71	0.1	0.1	10	1	1	1	0.8630	0.3506	2.2998
0.2	0.1	0.1	10	0.1	0.1	10	1	1	1	1.1462	0.4935	2.3471
0.2	0.1	0.1	0.71	0.5	0.1	10	1	1	1	0.8378	0.2850	2.3627
0.2	0.1	0.1	0.71	0.1	0.5	10	1	1	1	0.8951	0.3011	2.1404
0.2	0.1	0.1	0.71	0.1	0.1	25	1	1	1	0.7878	0.3556	3.8032
0.2	0.1	0.1	0.71	0.1	0.1	10	3	1	1	1.1693	0.2967	2.2374
0.2	0.1	0.1	0.71	0.1	0.1	10	1	2	1	1.0777	0.3415	2.2728
0.2	0.1	0.1	0.71	0.1	0.1	10	1	1	2	0.3633	0.4087	2.3875

The numerical results are analyzed through graphs and tabular values. The effect of various governing parameters on flow, heat and mass transfer are discussed in detail. The numerical results are depicted graphically in Figs. 1 – 16. Unless otherwise mentioned, the default values are pr = 0.71, Le=10, λ =1, m=1, M=1, Nt=Nb=Ec=0.1, R_1=100, R=0.2, γ=0.1 and δ=1 for subsequent results.

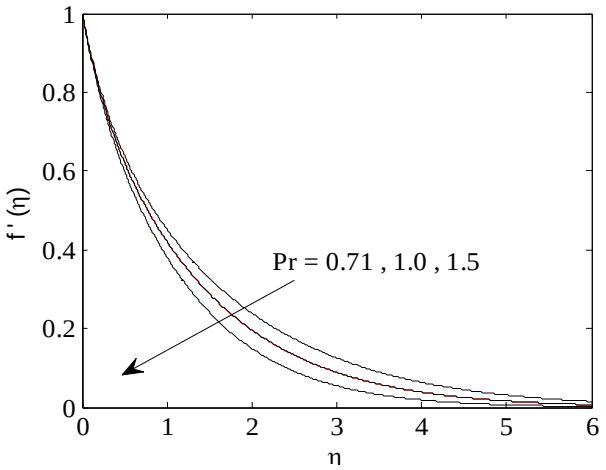

Fig.1. Variations of velocity profiles for different values of *Pr*.

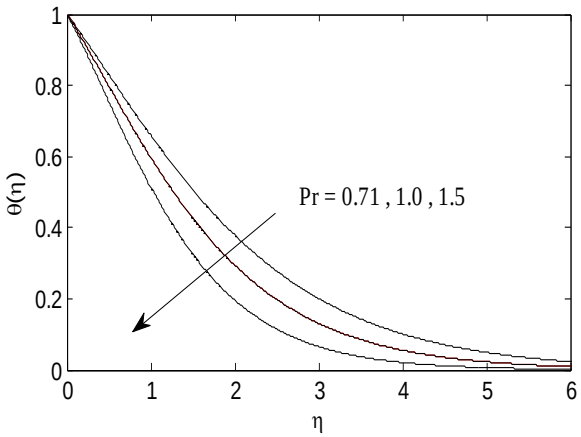

Fig.2. Variations of temperature profiles for different values of *Pr*.

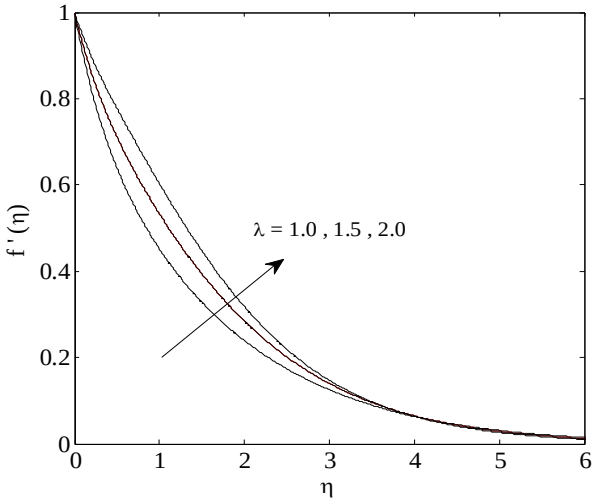

Fig.3. Variations of velocity profiles for different values of λ.

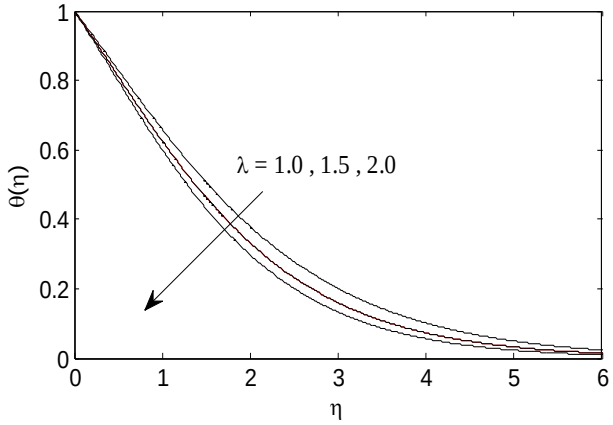

Fig.4. Variations of temperature profiles for different values of λ.

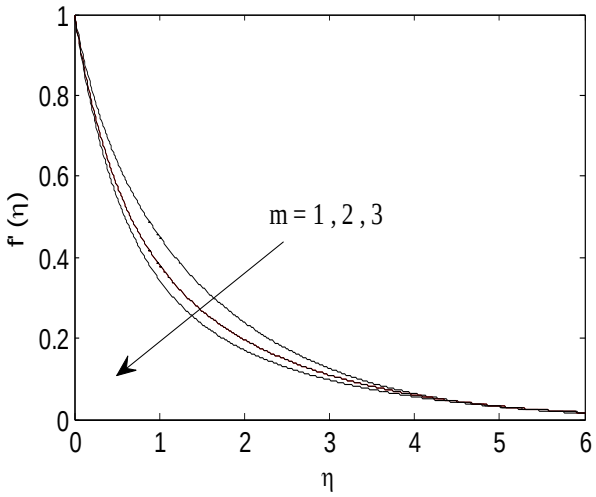

Fig.5. Variations of velocity profiles for different values of m.

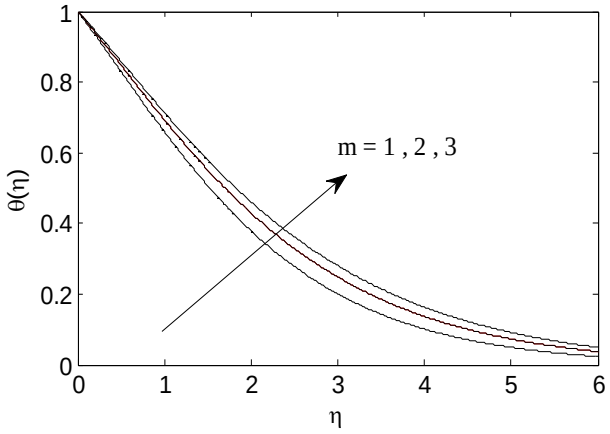

Fig.6. Variations of temperature profiles for different values of m.

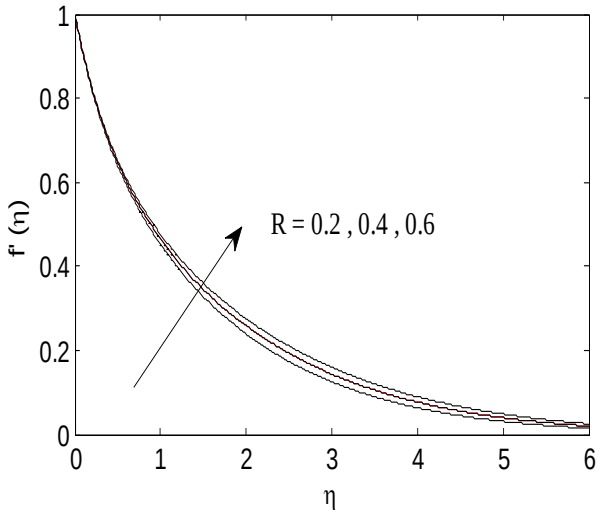

Fig.7. Variations of velocity profiles for different values of R.

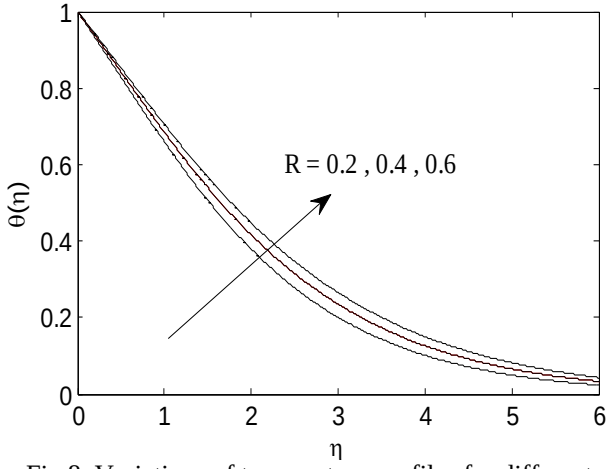

Fig.8. Variations of temperature profiles for different values of R.

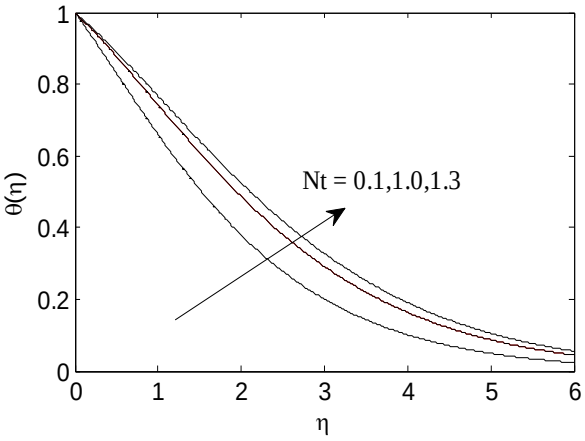

Fig.9. Variations of temperature profiles for different values of Nt.

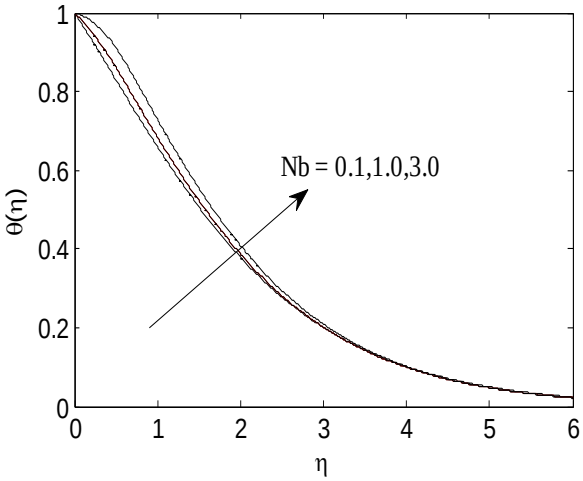

Fig.10. Variations of temperature profiles for different values of Nb.

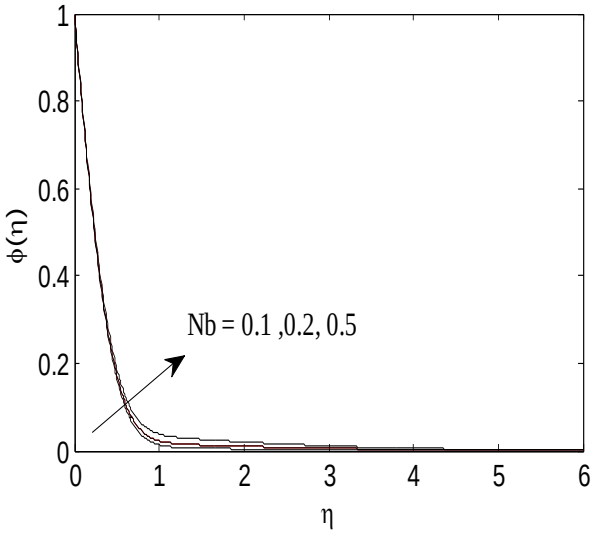

Fig.11. Variations of concentration profiles for different values of Nb.

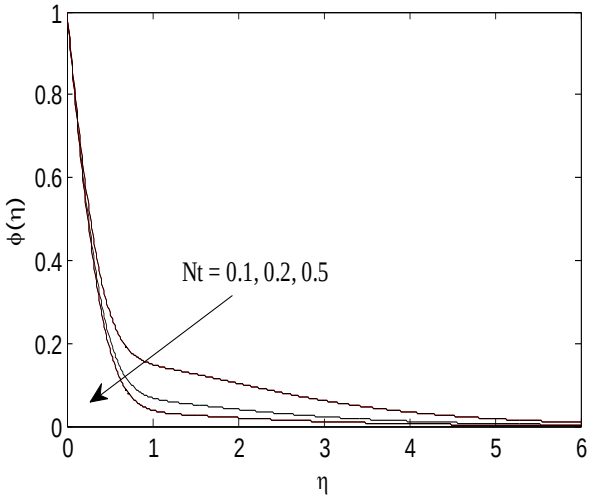

Fig.12. Variations of concentration profiles for different values of Nt.

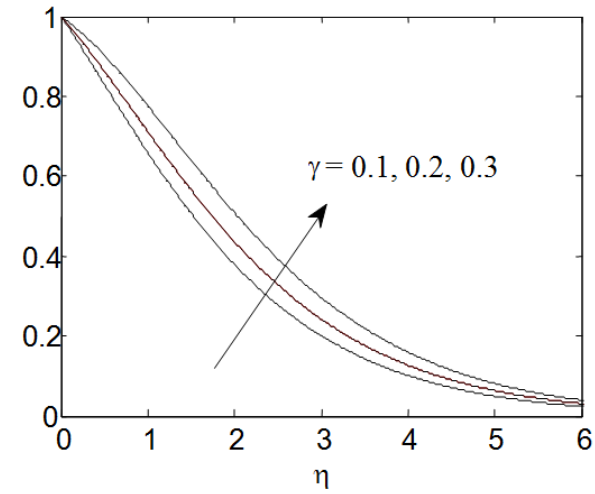

Fig.13. Variations of temperature profiles for different values of γ.

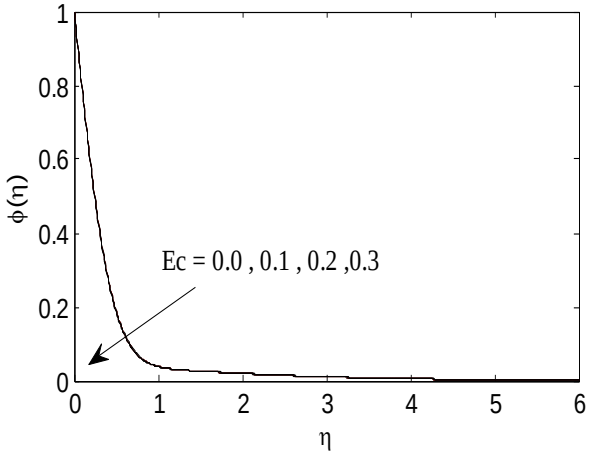

Fig.14. Variations of concentration profiles for different values of Ec

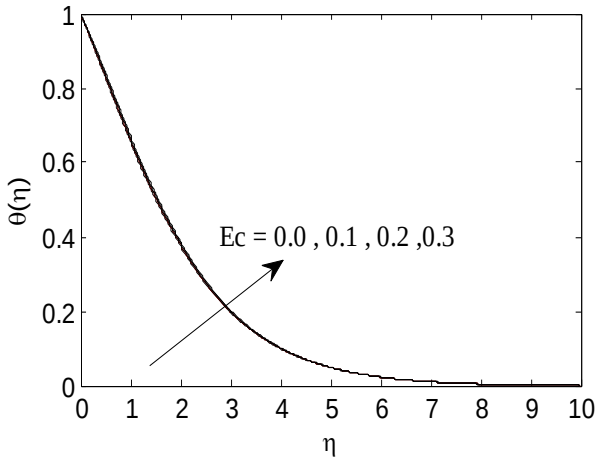

Fig.15. Variations of temperature profiles for different values of Ec.

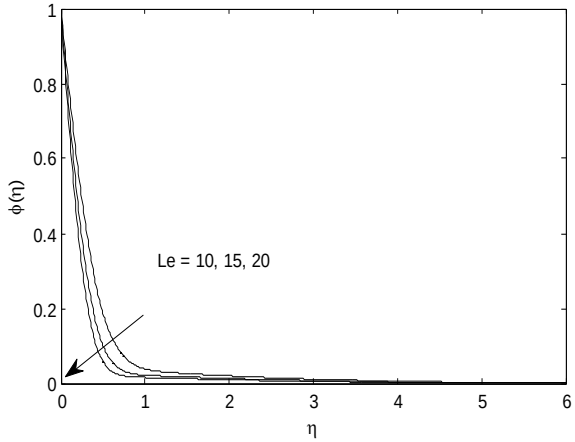

Fig.16. Concentration Profiles for different values of Le.

Table 3: Computations of velocity and temperature profiles for different values of δ.

δ	f ' (η)	θ(η)	f ' (η)	θ(η)	f ' (η)	θ(η)
	η=1		η=2		η=3	
1	0.9893191	0.9968845	0.9788352	0.9937519	0.9685441	0.9906027
2	0.9871958	0.9970185	0.9746858	0.9940174	0.9624634	0.9909972
3	0.9850163	0.9971677	0.9704243	0.9943126	0.9562146	0.9914354

Table 4: Computations of concentration profiles for different values of R.

R	Φ(η)	Φ(η)
	η = 2	η = 3
0	0.9549362	0.9324914
0.5	0.9544013	0.9316775
1.0	0.9540814	0.9311926

Table 5: Computations of concentration profiles for different values of λ

λ	Φ(η)	Φ(η)
	η = 2	η = 3
1	0.9546844	0.9321077
2.5	0.9524120	0.9286967
3.5	0.9511440	0.9267966

Table 6: Computations of concentration profiles for different values of γ

γ	Φ(η)	Φ(η)
	η = 2	η = 3
0	0.9555085	0.9333604
0.1	0.9546844	0.9321077
0.3	0.9527197	0.9291760

Figs. 1 and 2 show the effects of Prandtl number Pr on the velocity field f ' (η) and the temperature field θ(η) respectively. The Prandtl number Pr defines the ratio of momentum diffusivity to thermal diffusivity. It is noticed that an increase in the Prandtl number makes the fluid to be more viscous, which leads to a decrease in the velocity. It is noticed that an increase in the Prandtl number results in a decrease of the temperature, which in turn results in a decrease of the thermal boundary layer thickness. The reason is that smaller values of Pr are equivalent to increasing the thermal conductivities, and therefore heat is able to diffuse away from the heated stretching sheet more rapidly than for higher values of Pr. Hence in the case of smaller Prandtl numbers as the boundary layer is thicker and the rate of heat transfer is reduced.

The influence of the thermal buoyancy parameter λ, on velocity f ' (η) and temperature θ(η) are shown in Figs. 3 and 4 respectively. The positive (+ve) buoyancy force acts like a favorable pressure gradient and hence accelerates the fluid in the boundary layer. Hence velocity increases as λ increases. The temperature decreases as the thermal buoyancy parameter increases. This behavior is evident from Fig. 4.

Figs. 5 & 6 depict the influence of the stretching parameter m on velocity f ' (η) and temperature θ(η). It is noticed that increase in m results in decrease of velocity profile which is more pronounced for small values of m, whereas temperature profile increases with the increase of stretching parameter m. It is observed that the variation of the sheet temperature has a substantial effect on the thermal boundary layer. This effect is more pronounced when sheet temperature varies in the direction of highest stretching rate. Figs. 7 & 8 illustrate the effect of the thermal radiation parameter R on velocity and temperature respectively. When R increases, both velocity and temperature profiles increase. The radiation parameter R is responsible to thickening the thermal boundary layer. This enables the fluid to release the heat energy from the flow region and causes the system to cool. This is true because increasing the Rosseland approximation results in an increase in temperature. Thus lower values of R show a dominance of the thermal radiation over conduction. Consequently larger values of Rare indicative of larger values of radiative heat energy being powered into the system, causing a rise in θ(η).The temperature profiles for different values of thermophoresis parameter(Nt) and Brownian motion parameter(Nb) are shown in Figs. 9 & 10 respectively. It is noticed that the temperature increases with increasing values of Nb and Nt. The effects of Nb and Nt on the concentration profiles are represented in Figs. 11 & 12 respectively. It is noticed that as Nb increases the concentration increases and as Nt increases the concentration decreases. It is observed that positive Nt indicates a cold surface, while negative value indicates hot surface. The effect of heat source parameter γ on the temperature profiles is shown in Fig. 13. It is observed that as γ increases the temperature increases.

Figs. 14 and 15 show the effects of viscous dissipation parameter Ec on concentration profiles and temperature profiles. An increase in viscous dissipation parameter Ec enhances the temperature because the heat energy is stored in the liquid due to the frictional heating. The Eckert number Ec expresses the relationship between the kinetic energy in the flow and the enthalphy. It embodies the conversion of kinetic energy into internal energy by work done against the viscous fluid stresses. Greater viscous dissipative heat causes a rise in the temperature. This behavior is evident from Fig. 15. It is noticed that as Ec increases, the concentration profiles decrease. Fig.16 illustrates the effect of the Lewis number Le on the concentration. It is observed that the concentration decreases as the Lewis number increases. This is due to the fact that there is a decrease in the nanoparticle volume fraction boundary layer thickness with the increase in the Lewis number.

The influence of the solutal buoyancy parameter (δ) on velocity f'(η) and temperature θ(η) are shown in TABLE: 3. it is observed that an increase in solutal buoyancy parameter causes a decrease in velocity. The temperature increases as the solutal buoyancy parameter increases. TABLE: 4 shows the effect of the radiation parameter R

on the concentration. It is noticed that the concentration decreases as the radiation parameter increases. The influence of the thermal buoyancy parameters on the concentration field is shown in TABLE: 5. it is noticed that the concentration decreases as the thermal buoyancy parameter increases. TABLE: 6 show the effect of heat source parameter γ on the concentration profiles. It is observed that the concentration decreases as γ increases.

V. CONCLUSION

In present paper, effects of viscous dissipation, heat source parameters and thermal radiation on heat and mass transfer of free convective boundary layer flow of nanofluid over a nonlinear stretching sheet are analyzed. The influence of the various governing parameters on the velocity, temperature, concentration profiles is presented through graphs and tabular values.
The following conclusions are drawn.

- Velocity decelerates with an increase in the Prandtl number, solutal buoyancy parameter and stretching sheet parameter.
- Velocity accelerates with an increase in the thermal buoyancy, radiation and porosity parameters.
- There is a rise in the temperature with an increase in the Eckert number, solutal buoyancy parameter, stretching sheet parameter, radiation parameter, Nb, Nt, and γ.
- Temperature decreases with an increase in the Prandtl number and thermal buoyancy parameter.
- Concentration decreases with an increase in Ec, R, Nt and γ.
- Concentration increases with an increase in Nb, and λ.
- Skin friction coefficient increases with an increase in the Ec or Nb or Le or λ and decreases with an increase in R, Pr, Nt, m, δ, and γ.
- Nusselt number or Heat transfer rate rises with a rise in the Pr, Le and λ and it falls with an increase in the R, Nt ,m or δ, Ec , Nb and γ.
- Mass transfer rate increases with an increase in the R, Ec, Pr, Nb, Le, λ or γ and decreases with in increases in the Nt, m and δ.

REFERENCES

[1] Choi S: American Society of Mechanical Engineers, 1995, 99 – 105 , New York.
[2] Das S K, Putra N, Thiesen P, and Roetzel W: J. Heat Transfer, 2003, 125, pp. 567- 574.
[3] Buongiorno J: ASME J. Heat Transfer,2006, 128, 240 – 250.
[4] Buongiorno J, Hu :Nanofluid coolants for advanced nuclear power plants, Paper no. 5705, proceeding of ICAPP'05, Seoul, May 15- 19, 2005.
[5] Ahmad S and Pop I, International Communications in Heat and Mass Transfer, 2010, 37, pp. 987 – 991.
[6] Fekry M Hady, Fouad S Ibrahim, Sahar M Abdel-Gaied and Mohamed R Eid, Nanoscale Research Letters, 2012.
[7] Olanrewaju, P O, Olanrewaju, M A and Adesanya A O, International Journal of Applied Science and Technology, Vol. 2 No. 1: January 2012.
[8] Rohana Abdul Hamid, NorihanMd, Arifin, RoslindaMohdNazar , and loan Pop. Radiation effects on Marangoni boundary layer flow past a flat plate in nanofluid, Proceedings of the International Multiconfernce of Engineers and Computer Scientists,2011, Vol II, Hongkong.
[9] El- Aziz M A, Int. Commu. Heat and Mass Transf.,2009, 36, 521 – 524.
[10] Singh P, Jangid A, Tomel NS, Sinha D, Int. J. Info. And Math. Sci. 6,3. 2010.
[11] Gbadeyan JA, Olanrewaju, M A, and Olanrewaju, Australian Journal of Basic and Applied Sciences,2011, 5(9): 1323 – 1334.
[12] S Mohammed Ibrahim, Advancesin Applied Science Research, Pelagia Research Library, 2013,4(1), pp. 371 – 382.
[13] Sib Sankar Manna, Sanatan Das and RabindraNath Jana, Advances in Applied Science Research, Pelagia Research Library, 2012, 3(6): 3722 – 3736.
[14] Anandrao, Shivaiah S and NuslinSk, Advances in Applied Science Research, Pelagia Research Library, 2012, 3(3): 1663 – 1676.
[15] Kuznetsov V A and Nield D A, ,International Journal of Thermal Sciences, 2010, Vol. 49, no.2 , pp.243 – 247.
[16] Nield D A and Kuznetsov A V, International Journal of Heat and Mass Transfer,2009, Vol. 52, no. 25 – 26, pp. 5792 – 5795.
[17] Cheng P and Minkowycz W J ,Journal of Geophysical Research, 1977, 82, 2040 – 2044.
[18] Hossein Ali Pakravan, Mahmood Yaghoubi, International Journal of Thermal Sciences xxx, 2010, pp.1-9.
[19] Rana P, Bhargava R, Common Nonlinear SciNumerSimulat, 2011, 17(1): 212 – 226.
[20] Nadeem S , Lee C, Nanoscale Res Lett , 2012 , 7:94
[21] T Poornima and N. Bhaskar Reddy, Advances in Applied Science Research, 2013, 4(2): 190 – 202.
[22] Anwar M I, Khan I, Sharidan S. and Salleh M Z, International Journal of Physical Sciences, 2012 Vol. 7(26),pp 4081 – 4092.
[23] Kuznetsov AV, Nield DA (2010a). The Onset of Double-Diffusive nanofluid convection in a layer of a saturated porous medium. Transp. Porous Media. 85:941-951.
[24] Khan WA, Pop I (2010). Boundary-layer flow of a nanofluid past astretching sheet. Int. J. Heat Mass Transf. 53:2477-2483.
[25] Brewster MQ. Thermal radiatiative transfer and properties New York John Wiley (1992).
[26] Makinde OD, Olanrewaju PO, J.FluidsEng.Trans. ASME, 2010, 132: 044502- 1- 4.